Research Article Vol. 8, No. 3 / March 2021 / Optica 301

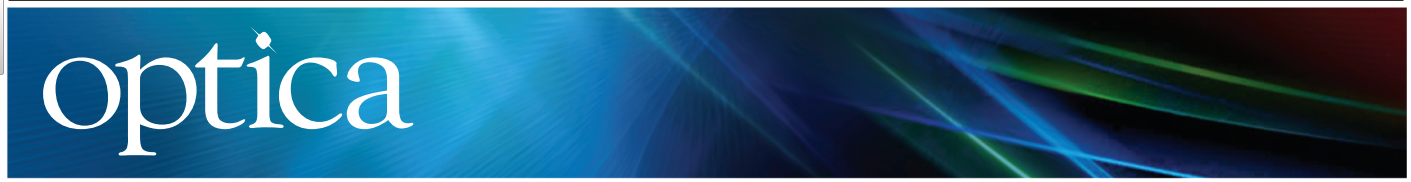

# Multiply charged vortex states of polariton condensates

SAMUEL N. ALPERIN[1] AND NATALIA G. BERLOFF[1,2,*]

[1]Department of Applied Mathematics and Theoretical Physics, University of Cambridge, Cambridge CB3 0WA, UK
[2]Skolkovo Institute of Science and Technology, Bolshoy Boulevard 30, bld.1, Moscow 121205, Russian Federation
*Corresponding author: N.G.Berloff@damtp.cam.ac.uk

Received 21 February 2020; revised 11 January 2021; accepted 11 January 2021 (Doc. ID 418377); published 1 March 2021

**The existence of quantized vortices is a key feature of Bose–Einstein condensates. In equilibrium condensates, only quantum vortices of unit topological charge are stable, due to the dynamical instabilities of multiply charged defects, unless supported by strong external rotation. Due to immense interest in the physics of these topological excitations, a great deal of work has been done to understand how to force their stability. Here we show that in photonic Bose–Einstein condensates of exciton–polariton quasiparticles pumped in an annular geometry, not only do the constant particle fluxes intrinsic to the system naturally stabilize multiply charged vortex states, but that such states can indeed form spontaneously during the condensate formation through a dynamic symmetry breaking mechanism. We elucidate the properties of these states, notably finding that they radiate acoustically at topologically quantized frequencies. Finally, we show that the vorticity of these photonic fluids is limited by a quantum Kelvin–Helmholtz instability, and therefore by the condensate radius and pumping intensity. This reported instability in a quantum photonic fluid represents a fundamental result in fluid dynamics.** 

https://doi.org/10.1364/OPTICA.418377

## 1. INTRODUCTION

From their macroscopic coherence, it follows that Bose–Einstein condensates (BECs) may support rotational flow only in the form of quantized vortices [1]. These vortices are thus topological in nature, and are characterized by a phase rotation of integer ($\ell$) steps of $2\pi$ around a phase singularity. However, while in principle quantized vortices may take on any topological charge, in practice, it is understood that only vortices of charge $\ell = \pm 1$ are dynamically stable: higher-order vortices quickly shatter into constellations of unit vortices due to the energetics of the system. This shattering process has been detailed theoretically and observed experimentally in the context of stationary, harmonically trapped atomic BECs [2–4]. The case is somewhat different for superharmonically trapped, rapidly rotated condensates, for which there exists a critical rotation rate above which the vorticity of the system becomes concentrated within a single effective core. This state, in which all vorticity is within a single effective core, has been called the *giant vortex* state by its first experimental observers [5,6]. Such a giant vortex is, therefore, different from a state in which there is a single point singularity with topological charge magnitude greater than one—*a multiply charged vortex*—however, in practice, it is often impossible to distinguish between the two. On one hand, the density in the vortex core is negligible, which hinders the resolution of singularity. On the other hand, the structure of interest is hydrodynamical, and thus has meaning only up to the length scales for which the hydrodynamical treatment applies. The classical field description being a long wavelength approximation of something that is in reality granular and nonclassical, the hydrodynamic description applies only down to the healing length. Singularities of like charge that are bound to within a healing length are thus, to any probe in the hydrodynamical regime, indiscernible from the theoretical *multiply charged vortex*. Thus, from here on, we find it useful to call all such vortex structures *multiply charged*.

In our study, we focus on a BEC away from the thermodynamical equilibrium supported by continuous gain and dissipation such as polariton [7], photon [8], or magnon [9,10] condensates. To be more specific, we use the example of polariton condensate; however, the results reported may be relevant to other nonequilibrium condensates. The exciton–polariton (polariton) is a bosonic quasiparticle composed of light (photons) and matter (excitons). Polaritons can be generated in optical semiconductor microcavities. In a typical experimental system, laser light is continuously pumped into the cavity to excite excitons (bound electron–hole pairs) in a semiconductor sample. The photons remain trapped in the cavity for some time, repeatedly being absorbed by the semiconductor to excite excitons, and then being re-emitted as the excitons decay. The excitons form superposition states (polaritons) with the photons, which behave as neither light nor matter. Due to the finite confinement times of the cavity photons, the polaritons in the condensate are themselves short lived. In this way, the polariton condensate is fundamentally different from other condensates: here, neither energy nor particle number need be conserved. Thus, while a polariton condensate may settle into a

*steady state* (a state in which the wavefunction is time invariant up to a global phase shift), such a state is one in which dissipation is balanced by particle gain. The corollary is that steady state flows are possible. It is well understood that the pattern-forming capabilities of nonequilibrium, nonconservative systems are richer than those of equilibrium, conservative systems [11], making the polariton condensate a fascinating object with which to explore the possibility of novel quantum hydrodynamical behaviors [12].

## 2. SPONTANEOUS FORMATION OF MULTIPLY CHARGED VORTICES

In this paper, we show theoretically that multiply charged vortex states can appear spontaneously and remain throughout the coherence time in a BEC of exciton–polariton quasiparticles excited by a ring-shaped laser profile, without the application of any external rotation, trapping potentials, or stirring. Previously, the spontaneous formation of multiply charged vortices of a given charge was theoretically proposed and experimentally realized in polariton condensates by pumping in an odd number of spots around a circle [13], or by the engineering of helical pumping geometries [14]. In the first case, the central vortex in this geometry is created driven by the antiferromagnetic coupling of the neighboring condensates and the frustration arising from their odd number. In the second case, the helical patterns are engineered so that the condensate is pumped explicitly with orbital angular momentum. Another recent proposal has shown that phase imprinted vorticity might remain concentrated at a localized mirror defect [15], in contrast to another recent work in which nonresonant pumping with a higher-order Laguerre–Gaussian beam resulted in the clear transfer of total vorticity, while failing to form a multiply charged vortex structure [16]. Yet other works have exploited the lack of simple connectedness of condensates confined to annular traps, in both equilibrium [17] and exciton–polariton condensates [18]; as in an annular condensate rotation does not necessitate a vortex defect. Interestingly, a central multi-charged vortex was observed in a numerical study of polariton condensates under the *weak* Mexican-hat-type pump (see supplemental material in [19]). There, the particle fluxes exist from the center outwards as the pumping profile peaks at the center. As the pumping intensity increases, the central vortex of small multiplicity (three in that case) breaks into the clusters of single-charge vortices trapped by the minima of the pumping potential. The multiply charged vortices we discuss here differ from these works in the geometry considered (ring-pumped trapped condensates, long coherence times), formation mechanism (probabilistic and spontaneous during condensation, away from the hot reservoir), and the vortex properties (vortices exist on the maximum density background and so are truly nonlinear in nature). We describe their formation, stability, and dynamics. The dynamics of two and more interacting multiply charged vortices are also studied. We find that our results apply for a wide range of possible experimental parameters, suggesting that these structures are general to ring-pumped trapped polariton BECs in the strong coupling regime.

The dynamics of the polariton BEC in the mean field are described by the complex Ginzburg–Landau equation (cGLE) coupled to a real reservoir equation representing the bath of hot excitons in the sample, nonresonantly excited by the spatially resolved laser pump profile $P(\mathbf{r})$ [20–24]:

$$i\hbar\partial_t\psi = -\frac{\hbar^2}{2m}(1 - i\hat{\eta}N_R)\nabla^2\psi + U_0|\psi|^2\psi + g_R N_R\psi + \frac{i\hbar}{2}(R_R N_R - \gamma_C)\psi, \tag{1}$$

$$\partial_t N_R = P - (\gamma_R + R_R|\psi|^2)N_R, \tag{2}$$

in which $\psi$ represents the condensate wavefunction, $N_R$, and the exciton reservoir density. $U_0$ and $g_R$ give the polariton–polariton and exciton–polariton interaction strengths, and $R_R$ and $\hat{\eta}$ represent the scattering and diffusion rates, respectively. The effective mass of the polariton is given by $m$. Finally, the loss rates of excitons and polaritons are described by $\gamma_C$ and $\gamma_R$, respectively. To rewrite these equations in a more amenable, nondimensional form, we employ the transforms $\psi \to \sqrt{\hbar R_R/2U_0 l_0^2}\psi$, $t \to 2l_0^2 t/\hbar R_R$, $r \to \sqrt{\hbar l_0^2/(m R_R)}r$, $N_R \to N_R/l_0^2$, and $P \to R_R P/2\hbar l_0^2$, and we define the nondimensionless parameters $g = 2g_R/R_R$, $b_0 = 2\gamma_R l_0^2/\hbar R_R$, $b_1 = R_R/U_0$, $\eta = \hat{\eta}/l_0^2$, $\gamma = \gamma_C l_0^2/R_R$, and $\gamma = \gamma_C l_0^2/R_R$, where we set $l_0 = 1$ μm. This yields [25]

$$i\partial_t\psi = -(1 - i\eta N_R)\nabla^2\psi + |\psi|^2\psi + g N_R\psi + i(N_R - \gamma)\psi, \tag{3}$$

$$\partial_t N_R = P - (b_0 + b_1|\psi|^2)N_R. \tag{4}$$

Polaritons can be confined all-optically by shaping the excitation laser beam. By using spatial light modulators to shape the optical excitation, ring-shaped confinements were generated with condensates forming inside the ring [26,27], and have been predicted to support the spontaneous formation of unit vortices [28]. Long-lifetime polaritons in ring traps are emerging as a platform for studies of fundamental properties of polariton condensation largely decoupled from the excitonic reservoir and therefore having significantly larger coherence times [29–32]. We represent the profile of the ring pump by a Gaussian annulus of the form $P(r, \theta, t) = Pe^{-\alpha(r-r_0)^2}$ with inverse width $\alpha$ and radius $r_0$, which excites local quasiparticles that then flow outward. The closed-loop pump geometry has two major implications. The first is that the condensation threshold is first achieved not where the sample is pumped, but *within* the borders of the pumping ring. This results in the effective spatial separation of Eqs. (3) and (4), which makes the parameters related to excitonic reservoirs such as $b_0$, $b_1$, and $g$ irrelevant to the condensate dynamics up to a change in pump strength. The second and most critical implication of the ring pump geometry is the existence of constant fluxes towards the center of the ring. Such fluxes carry the matter together with spontaneously formed vortices and force vortices to coalesce.

It is well known that vortices can form during the rapid condensation of a Bose gas via the Kibble–Zurek mechanism [33–42]. However, in our system, there exists a different mechanism of spontaneous defect generation that requires a relatively *slow* condensate formation. Due to the inward flow of particles in our system, the condensation threshold is reached first in the center of the system. Assuming a large enough ratio of new particle flow to dissipation, this young condensate will grow into a relatively uniform disk within the boundary of the pump. However, in between these two stages, radial matter wave interference is to be expected, with higher frequency during the early stages of condensation. The zeros of the radial interference pattern are well studied under a different name: the dark ring soliton [11,43,44]. As has been

shown previously, these dark solitons are unstable to transverse ("snake") perturbations, and break apart into pairs of unit vortices of opposite charge [45,46]. Thus, for a slowly condensing system, it is reasonable to expect that these solitons have enough time to break down to produce a chaotic array of vortex singularities. This process resembles a two-dimensional case of the collapsing bubble mechanism of vortex nucleation [47]. As the condensation process completes and the vortex turbulence decays, there is some finite chance of the condensate being left with a net topological charge, as vortex pairs may unbind near the boundary, and one or the other may leave to annihilate with its image. These like-charged vortices would then coalesce in the center of the condensate.

Direct numerical integration of Eqs. (3) and (4) not only confirms that this process can take place, but that for low pump power, the condensate takes on a net topological charge more often than not. (Fourth order Runga–Kutta integration is used. The initial wavefunction is set to a profile of low amplitude random noise. All simulations are repeated for many of these profiles.) We reiterate that this coalescence of vortices exists despite the lack of external rotation or sample nonuniformity. Repeating the numerical experiment with many iterations of random initial wavefunction noise, we find multiply charged vortex states of stochastic sign and magnitude. The average topological charge magnitude is found to depend significantly on the radius of the pump ring, increasing for larger radii. An example of these dynamics is presented in Fig. 1, which shows the main steps in the process by which the condensate spontaneously adopts a topological charge of two: the formation of a central condensate surrounded by annular discontinuities in Fig. 1(a), the breakdown of an annular discontinuity into vortex pairs in Fig. 1(b), vortex turbulence in Fig. 1(c), and the final bound vortex state in Fig. 1(d). For Fig. 1, we use the system parameters $\eta = 0.3$, $\gamma = 0.05$, $g = 1$, and $b_0 = 1$, $b_1 = 6$, but the result was found not to depend sensitively on these choices; up to a rescaling of pump strength, this behavior was reconfirmed for a large range of sample parameters: $g \in [0.1 - 2]$, $b_0 \in [0.01 - 10]$ for $\gamma \in [0.05 - 0.1]$, and for all reasonably physical values of $\eta$ (including $\eta = 0$.)

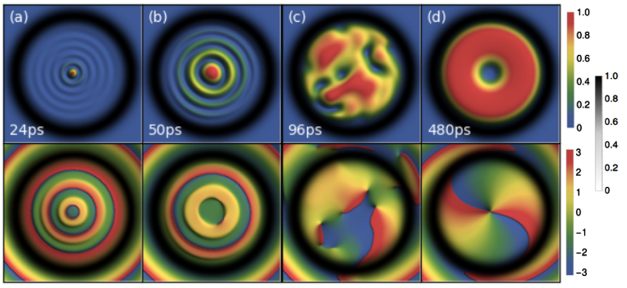


**Fig. 1.** Spontaneous formation of a multiply charged quantum vortex in a ring pumped polariton condensate by numerical integration of Eqs. (3) and (4). Density (top row) and phase (bottom row) snapshots are shown at various stages of the condensate formation. For clarity, each density profile is rescaled to unit maxima. The pumping profiles are superposed in black (in units of P), showing the spatial separation between the pump and the condensate. (a) At the beginning of the condensate formation, due to the pump geometry, matter wave interference leads to annular zeros in the wavefunction. (b) These ring singularities are unstable to dynamical instability, become asymmetrical and can be observed to break into more stable unit vortices as the condensate continues to develop. (c) The condensate fills a disk shaped region with near uniformity within the ring pump, but remaining vortices interact chaotically. The vortex turbulence eventually decays, leaving a net topological charge [48,49]. Repeating these simulations with different random initial conditions, the magnitude and sign of the final vorticity vary. Here, $P = 5$ and $r_0 = 11.5$ μm.

An advantage of the spatial separation of the condensate from the reservoir in ring-pumped geometry is in the enhanced coherence time that exceeds the individual particle lifetime by three orders of magnitude [50]. Therefore, spontaneously created multiply charged vortices might soon be observable in single-shot experiments within one condensate realization. However, for now, only the average wavefunctions of many iterations of the stochastic condensate formation are observable in experiment. In a perfectly uniform sample, one would expect an equal chance of the stochastic formation of vortex charges of either handedness, which would cancel in the experimentally observable mean wavefunction. However, it has been established in experiments that the slight inhomogeneities inherently present in all physical samples act to favor one handedness over the other [13]. Thus, the only experimental observable is the mean *magnitude* of the vorticity distribution. This magnitude is well above zero for a wide range of parameters, making the experimental observation of this effect highly feasible within the current state of the art. (For example: mean vorticity amplitudes determined from direct simulations of Eqs. (3) and (4) for pump radius 12 μm tend linearly from 2.5 to 4.9 as the pump strength is decreased from $P = 9$ to $P = 5$.)

## 3. VORTEX IMPRINTING

Another way to study multiply charged vortices is to imprint them explicitly upon a fully formed, uniform condensate [51]. This allows for the study of the structure and dynamics of carefully controlled systems of vortices. To model the result of experimental pulsed phase imprinting, we first model the formation of fully developed non-singular condensate disks. To prevent the spontaneous formation of vortices by the process described above, a relatively strong pump amplitude is used, so that the condensate forms too quickly for the decay of ring singularities into vortices. After the background condensate is formed, phase singularities are imprinted instantaneously, and their dynamics are observed. To first understand the structure of isolated multiply charged vortices, we imprint a series of condensates with different topological charges, and allow these structures to form steady states. When imprinted in equilibrium BEC, multiply charged vortices quickly break into vortices of a single unit of quantization [52].

From the spatial separation of the condensate and the reservoir, the reservoir density is negligible near the central core of the multiply charged vortex, so that Eq. (3) takes the familiar form of the damped nonlinear Schrödinger equation (dNLSE): $i\partial_t\psi = -\nabla^2\psi + |\psi|^2\psi - i\gamma\psi$.

Under the Madelung transformation $\psi = \mathcal{A}\exp[iS - i\mu t]$, where $\mu$ is the chemical potential, the velocity is the gradient of the phase $S$: $\mathbf{u} = \nabla S$, the density is $\rho(r) = \mathcal{A}^2$, and the imaginary part of the dNLSE yields $\nabla\cdot(\rho\mathbf{u}) = -\gamma\rho$. Except for a narrow spatial region where the density heals itself from zero to the density of the vortex-free state, the density is almost a constant, so the radial component of the velocity becomes $u_r = -\gamma r$. The real part of the dNLSE reads

$$\partial_r^2\mathcal{A} + \partial_r\mathcal{A}/r + (\mu - \mathbf{u}^2 - \mathcal{A}^2)\mathcal{A} = 0, \tag{5}$$

which coincides with the corresponding steady state equation for the equilibrium condensates where the velocity profile plays the role of the external potential. We therefore expect the structure

of the vortices to be similar to those in equilibrium condensates, with the external potential given by $\mathbf{u}^2$. Close to the center of the condensate, the velocity becomes $\mathbf{u} = -\gamma r\hat{r} + \frac{\ell}{r}\hat{\theta}$, where $\hat{r}$ and $\hat{\theta}$ are unit vectors in polar coordinates. When this expression for $\mathbf{u}$ is substituted into Eq. (5), it becomes the equation on the vortex amplitude in the center of the harmonic trap, where $\gamma$ characterizes the frequency of the "trap." In the vortex core, for small $r$, the centrifugal velocity dominates the radial velocity, so the equation on the rescaled amplitude $A = \mathcal{A}/\sqrt{\mu}$, with $\tilde{r} = \sqrt{\mu}r$, becomes

$$\partial_{\tilde{r}^2} A + \partial_{\tilde{r}} A/\tilde{r} + \left(1 - \frac{\ell^2}{\tilde{r}^2} - A^2\right) A = 0. \tag{6}$$

The profiles $A$ take the approximate form

$$A = \frac{\tilde{r}^{|\ell|}}{(\tilde{r}^n + w)^{|\ell|/n}}, \tag{7}$$

with parameters $w$ and $n$, in which we incorporated the power expansion behavior of the amplitude $A \sim \tilde{r}^{|\ell|}$ as $\tilde{r} \to 0$. Figure 2 shows the amplitude cross-section profiles of stable giant vortices with different topological charges $\ell \in \{1, 2, \ldots, 10\}$ as the solutions to Eq. (6), along with Eq. (7), showing a compelling fit between vortex profiles seen in the full numerical simulations of the coupled condensate–reservoir system (without an external trap) and those of the steady state solutions of an equilibrium condensate under harmonic trapping, as predicted by our theory.

We have shown above that the inward fluxes necessitated by the closed pumping geometry result in an effective trapping potential—independent of any effective trapping from the reservoir near the edge of the condensate—which drives the vortices closer together. Our analysis, which shows that the forces from the inward fluid fluxes overcome the topological repulsion of like-signed vortices, applies when the condensate is nearly uniform, which is the case until the vortices begin to overlap. At this stage, there is further interaction between vortices: it has long been understood that in nonequilibrium systems, the topological repulsion of like-signed vortices can be balanced due to the nontopological force emerging from the effective variations in the supercriticality stemming from the density decrease surrounding the defects [53]. The variable-supercriticality force is negligible until the vortices are close enough for significant overlap between their associated density structures. In our system, the radial flux forces bring the vortices of like sign to within the regime at which they may bind to form a multiply charged vortex.

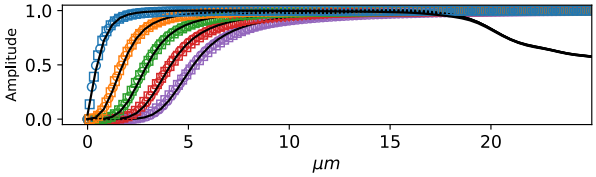


**Fig. 2.** Wavefunction amplitude cross sections $\sqrt{\rho(r)}$ of multiply charged vortices. For clarity, and without loss of generality, we show only odd topological charges less than $\ell = 10$. Profiles from the full numerical integration of Eqs. (3) and (4) (normalized) for $r_0 = 20$ μm, $P = 12$, and $\gamma = 0.3$ are shown in black, and illustrate the decay of the condensate near the pump ring. The numerical solutions to the reduced equation Eq. (6) are marked by circles colored by charge, and the corresponding fits to the ansatz Eq. (7) by squares with matching colors. From these fits, we can write the approximate parameterization of Eq. (6) as $n(\ell) = (1.1)\ell^{1.6} - 2.8$ and $w(\ell) = 2.3 + (0.6)\ln(\ell)$).

## 4. VORTEX MERGER

Next we consider the arrangements of multiple multiply charged vortices imprinted away from the trap center and brought together by the radial fluxes. Figure 3 shows two examples of the coalescence dynamics of imprinted phase defects. In the first case, three unit vortices coalesce while moving in inward spirals towards the center of the condensate, where there is no net lateral flow. In the second case, which shows the coalescence of two doubly charged vortices, it is observed that both doubly charged vortices hold together for a while before merging in the center to form a single vortex of multiplicity four. These results are found to be repeatable for a wide range of system parameters, suggesting that this behavior is to be expected for any system parameter that allows the formation of a trapped condensate within a ring pump. We note that in this system, the center of the condensate corresponds to the location of maximum background fluid density, in stark contrast to systems designed to collect virtual vorticity into a low-density area [17].

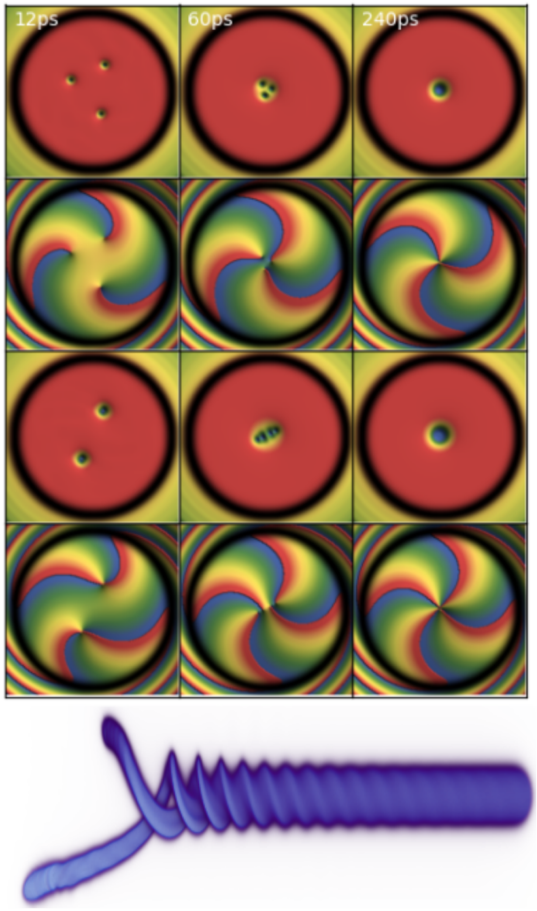


**Fig. 3.** From top: density (first row) and phase (second row) resolved dynamics of three unit vortices of like charge in a condensate formed within the boundary of an annular pump (green). Over time, the three vortices approach each other in an inward spiral, eventually merging to an inter-singularity length scale less than the healing length of the condensate. Density (third row) and phase (fourth row) of two doubly charged vortices (each having topological charge $n = 2$), which over time merge into a single fourth-order vortex. Here, $P = 10$ and $r_0 = 15$ μm. Color scales are the same as in Fig. 1. At bottom, a density isosurface of the two merging second-order vortices, with time shown along the horizontal axis, from 12 ps (left) to 240 ps (right).

As two (or more) vortices merge while spiraling around the center, they excite density waves in the otherwise uniform background fluid. These acoustic excitations are long lived, and take on a frequency set by the angular frequency of the vortex spiral. For well-separated vortices, this frequency increases consistently as time progresses and their separation shrinks. However, as the vortices begin to share a core, these dynamics become even more complicated, and the new physics dominated by the processes in the vortex core emerges [54].

Figure 4 shows the relative amplitudes of the density waves radiated during the motion of two vortices of unit charge imprinted with a large initial separation. The average frequency of acoustic radiation is found to increase with time at a fixed rate until the vortex cores begin to overlap (left vertical line). During this phase, the frequency distribution narrows, and the average radiation frequency increases linearly at a much lower rate than in the well-separated vortex regime. This continues until the singularities within the core overlap within a healing length (right vertical line), after which a fixed narrow band of acoustic radiation is emitted.

Of course, multiply charged vortices may also collide: we find that from merger of two equal multiply charged vortices of increasing topological charge, the characteristic acoustic resonances have decreasing frequency, in the near-terahertz regime. This is because the effective mass of the vortex increases with topological charge, so that vortices of larger multiplicity orbit more slowly. As expected, we see that in contrast, when multiple singly charged vortices placed evenly about a common radius merge, they emit higher frequency radiation as the number of unit vortices is increased. Once the multiply charged vortex has formed and is allowed to settle, low-energy density perturbations can be applied to the condensate. To model this, we simulate the effect of a small Gaussian laser pump pulse centered on the vortex. The observed effect is the

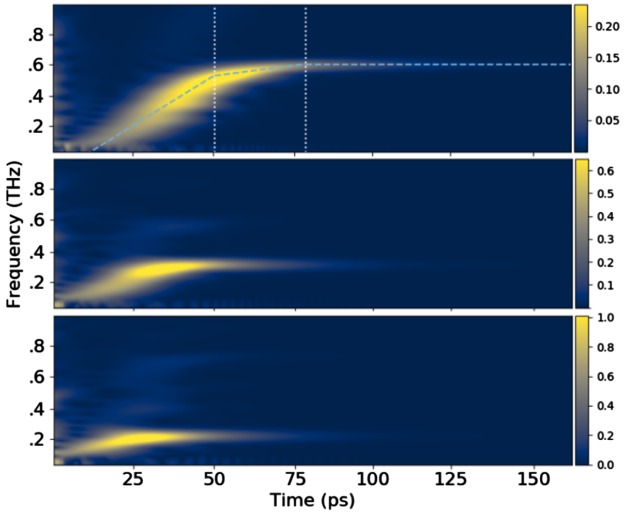


**Fig. 4.** Power spectral density of acoustic waves radiated by the approach and merger of two vortices, resolved in time–frequency space. Top panel shows the merger of two unit vortices, and vertical lines mark the time of transition from well-separated vortices to vortices sharing a common low-density core (left) and the time at which the singularities have merged to within a healing length (right). Middle and bottom panels show the acoustic spectra of two merging doubly charged vortices (middle) and two merging triply charged vortices (bottom). The ring pump radius is 20 μm. In the case of two single vortices, one vortex is imprinted at the condensate center, and the other at a distance of 18 μm from the center. In the cases of two multiply charged vortices, both vortices are imprinted 18 μm from the center.

emission of an acoustic energy pulse at the characteristic frequency of the vortex, as is seen from the merger of the equivalent number of unit vortices. As in any physical system, there exist many small perturbations due to intrinsic disorder, and it is likely that multiply charged vortices in a real system are regularly being excited and emitting acoustic radiation.

*Kelvin–Helmholtz instability.* Next we will establish the limit on the vortex multiplicity that the trapped condensate can support. This limit is set by the maximum counterflow velocity that can be supported between the condensate and the reservoir, therefore determined by the onset of Kelvin–Helmholtz instability (KHI). KHI is the dynamical instability at the interface of two fluids when the counterflow velocity exceeds a criticality. It appears in a variety of disparate systems, both classical and quantum, but has never been discussed in the context of polaritonic systems. In quantum fluids, KHI manifests itself via nucleation of vortices at a counterflow velocity exceeding the local speed of sound: $v_c = \sqrt{\frac{U_0\rho}{m}}$. It has been extensively studied for the interface between different phases of $^3$He [55], two components in atomic BECs [56], or for the relative motion of superfluid and normal components of $^4$He [57,58]. In the trapped condensates considered here, the counterflow is that between the condensate of radius $R$ (which rotates with velocity $\frac{\hbar}{m}\frac{|\ell|}{R}$ at the boundary) and the reservoir particles along the ring, which are stationary. Thus, it is expected that KHI should be initiated when the topological charge of the multiply charged vortex state is high enough that the velocity of condensate particles at the ring pump radius reaches $v_c$. Thus, the maximum topological charge $\ell_c$ allowed is set by

$$|\ell_c| = \frac{\sqrt{R^2 m U_0 \rho}}{\hbar}. \tag{8}$$

Figure 5 shows Eq. (8) (dashed line) along with the critical topological charges found by direct numerical integration of Eqs. (3) and (4) (dots). In these numerical experiments, we begin with a fully developed, vortex-free condensate. A unit topological charge is imprinted in the center of the condensate, and the system is allowed to settle, before another unit charge is added. This process is repeated until the onset of KHI leads to the vortex nucleation followed by annihilation of vortex pairs and, therefore, by a reduction in the topological charge of the system. This dynamical process is shown in Fig. 6. We note that the question of the critical velocity in superfluids is always a subtle one. Even in the simplest case of a homogeneous superflow around a 2D disk (first studied in [59]), both numerical and experimental data fluctuate significantly around the analytical prediction of criticality [60]. In contrast, we have a much more complicated nonequilibrium system on a nonuniform background with a nonuniform reservoir, and our

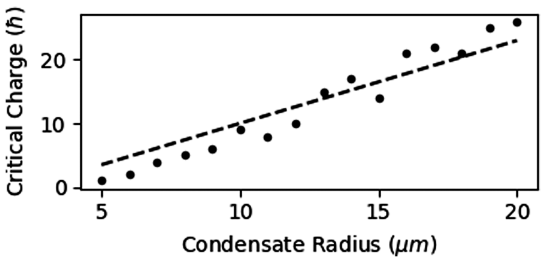


**Fig. 5.** Critical topological charge at which the KHI sets in, as a function of pump radius. This is obtained by the direct numerical simulations of Eqs. (3) and (4). The dashed line represents the theoretical expectation of Eq. (8).

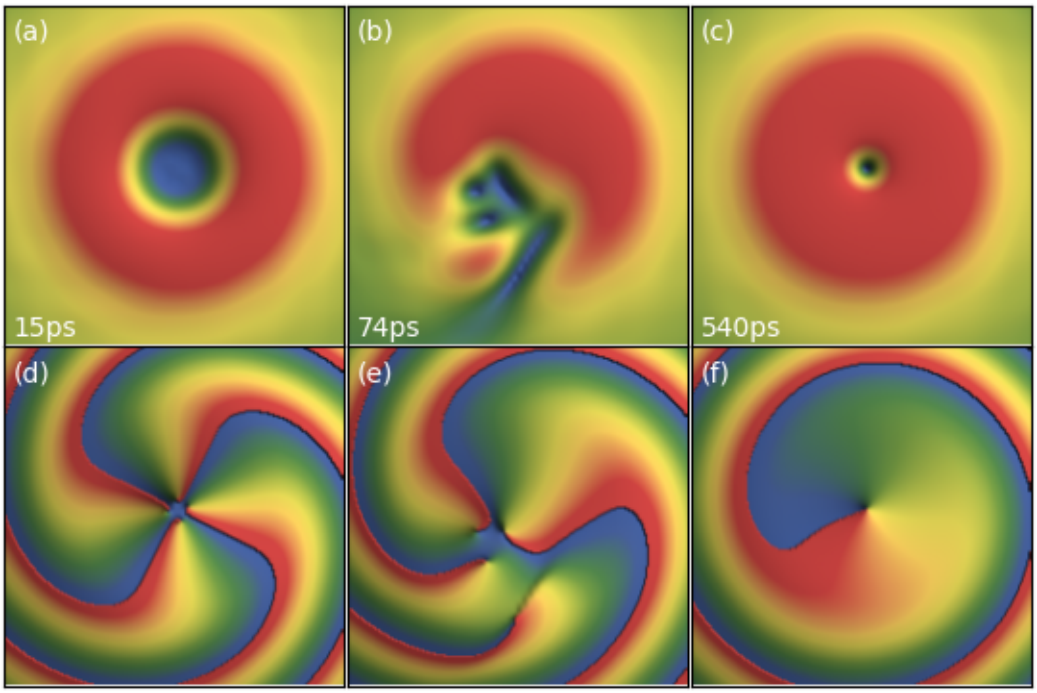


**Fig. 6.** For a great enough topological charge (compared to the size of the condensate), the rotational flow at the boundary of the condensate reaches the critical velocity for the Kelvin–Helmholtz instability to set in, which results in a reduction in topological charge via the nucleation of new vortices, with charges opposite to that of the multiply charged vortex and further pair annihilation. Shown are density profiles from a direct simulation of Eqs. (3) and (4) exhibiting this process (radius 7 μm, $P = 10$). The initial topological charge is imprinted one quantum at a time, and the dynamics observed. After the fourth quantum of rotation is imprinted, the system loses stability and expels some rotation through the KHI mechanism, ending with unit topological charge.

numerical data as compared to the analytical estimate are rather accurate and show the correct trend.

## 5. CONCLUSION

In conclusion, we have shown that exciton–polariton condensates excited by an annular pump can spontaneously rotate despite a uniform sample and no angular momentum applied, forming multiply charged vortices. The formation, dynamics, and structure of these vortices were studied. We emphasize that the KHI mechanism is quite specific to the ring-like pumping configuration we considered. In gain-dissipative condensate systems, particle fluxes exist even in the steady state, connecting the regions where they are predominantly created to the regions where they are predominantly dissipated. With the ring-like pumping, the fluxes are oriented strictly towards the center, stabilizing the multiply charged vortex while preventing the formation of localized vortex clusters elsewhere. When other pumping profiles are considered, a more complicated flux distribution emerges. In some localized parts of the sample, radial fluxes may exist similar to our ring-like pumping, but much weaker and less controllable. This may create conditions for the formation of multiply charged vortices, but of rather small multiplicity and that are quickly destroyed by the small changes in parameters (e.g., pumping intensity or the pumping spot size). For instance, the Mexican hat pumping profile in [19] gives rise to outward particle fluxes from the center in addition to inward fluxes from the annular pump, so a vortex of small multiplicity (two or three) is destroyed as the pumping intensity is increased, instead bringing about clusters of vortices stabilized where the fluxes from the center meet the radially inward fluxes. This destruction of the multiply charged vortices in this and similar cases cannot be attributed to KHI.

**Disclosures.** The authors declare no conflicts of interest.

## REFERENCES

1. R. P. Feynman, "Chapter II: Application of quantum mechanics to liquid helium," in *Progress in Low Temperature Physics* (Elsevier, 1955), Vol. **1**, pp. 17–53.
2. S. Inouye, S. Gupta, T. Rosenband, A. Chikkatur, A. Görlitz, T. Gustavson, A. Leanhardt, D. Pritchard, and W. Ketterle, "Observation of vortex phase singularities in Bose-Einstein condensates," Phys. Rev. Lett. **87**, 080402 (2001).
3. Y.-I. Shin, M. Saba, M. Vengalattore, T. Pasquini, C. Sanner, A. Leanhardt, M. Prentiss, D. Pritchard, and W. Ketterle, "Dynamical instability of a doubly quantized vortex in a Bose-Einstein condensate," Phys. Rev. Lett. **93**, 160406 (2004).
4. P. Engels, I. Coddington, P. Haljan, V. Schweikhard, and E. A. Cornell, "Observation of long-lived vortex aggregates in rapidly rotating Bose-Einstein condensates," Phys. Rev. Lett. **90**, 170405 (2003).
5. U. R. Fischer and G. Baym, "Vortex states of rapidly rotating dilute Bose-Einstein condensates," Phys. Rev. Lett. **90**, 140402 (2003).
6. A. L. Fetter, B. Jackson, and S. Stringari, "Rapid rotation of a Bose-Einstein condensate in a harmonic plus quartic trap," Phys. Rev. A **71**, 013605 (2005).
7. J. Kasprzak, M. Richard, S. Kundermann, A. Baas, P. Jeambrun, J. Keeling, F. Marchetti, M. Szymańska, R. André, J. Staehli, and V. Savona, "Bose–Einstein condensation of exciton polaritons," Nature **443**, 409–414 (2006).
8. J. Klaers, J. Schmitt, F. Vewinger, and M. Weitz, "Bose–Einstein condensation of photons in an optical microcavity," Nature **468**, 545–548 (2010).
9. V. Demidov, O. Dzyapko, S. Demokritov, G. Melkov, and A. Slavin, "Observation of spontaneous coherence in Bose-Einstein condensate of magnons," Phys. Rev. Lett. **100**, 047205 (2008).

10. P. Nowik-Boltyk, O. Dzyapko, V. Demidov, N. Berloff, and S. Demokritov, "Spatially non-uniform ground state and quantized vortices in a two-component Bose-Einstein condensate of magnons," Sci. Rep. **2**, 482 (2012).
11. L. M. Pismen, *Patterns and Interfaces in Dissipative Dynamics* (Springer, 2006).
12. S. N. Alperin and N. G. Berloff, "Formation and dynamics of quantum hydrodynamical breathing ring solitons," Phys. Rev. A **102**, 031304 (2020).
13. K. Kalinin, M. Silva, J. D. Töpfer, W. Langbein, N. G. Berloff, and P. G. Lagoudakis, "Giant vortices of controlled multiplicity in polariton lattices," arXiv preprint arXiv:1710.03451 (2017).
14. R. Dall, M. D. Fraser, A. S. Desyatnikov, G. Li, S. Brodbeck, M. Kamp, C. Schneider, S. Höfling, and E. A. Ostrovskaya, "Creation of orbital angular momentum states with chiral polaritonic lenses," Phys. Rev. Lett. **113**, 200404 (2014).
15. D. D. Solnyshkov, C. Leblanc, S. V. Koniakhin, O. Bleu, and G. Malpuech, "Quantum analogue of a Kerr black hole and the Penrose effect in a Bose-Einstein condensate," Phys. Rev. B **99**, 214511 (2019).
16. M. Kwon, B. Y. Oh, S. Gong, J. Kim, H. K. Kang, S. Kang, J. D. Song, H. Choi, and Y. Cho, "Direct transfer of light's orbital angular momentum onto a nonresonantly excited polariton superfluid," Phys. Rev. Lett. **122**, 045302 (2019).
17. M. Cozzini, B. Jackson, and S. Stringari, "Vortex signatures in annular Bose-Einstein condensates," Phys. Rev. A **73**, 013603 (2006).
18. V. A. Lukoshkin, V. K. Kalevich, M. M. Afanasiev, K. V. Kavokin, Z. Hatzopoulos, P. G. Savvidis, E. S. Sedov, and A. V. Kavokin, "Persistent circular currents of exciton-polaritons in cylindrical pillar microcavities," Phys. Rev. B **97**, 195149 (2018).
19. F. Manni, T. C. H. Liew, K. G. Lagoudakis, C. Ouellet-Plamondon, A. André, V. Savona, and B. Deveaud, "Spontaneous self-ordered states of vortex-antivortex pairs in a polariton condensate," Phys. Rev. B **88**, 201303 (2013).
20. I. Carusotto and C. Ciuti, "Quantum fluids of light," Rev. Mod. Phys. **85**, 299–366 (2013).
21. M. Wouters and I. Carusotto, "Excitations in a nonequilibrium Bose-Einstein condensate of exciton polaritons," Phys. Rev. Lett. **99**, 140402 (2007).
22. J. Keeling and N. G. Berloff, "Spontaneous rotating vortex lattices in a pumped decaying condensate," Phys. Rev. Lett. **100**, 250401 (2008).
23. M. Wouters, T. Liew, and V. Savona, "Energy relaxation in one-dimensional polariton condensates," Phys. Rev. B **82**, 245315 (2010).
24. M. Wouters, "Energy relaxation in the mean-field description of polariton condensates," New J. Phys. **14**, 075020 (2012).
25. K. P. Kalinin and N. G. Berloff, "Simulating Ising and n-state planar Potts models and external fields with nonequilibrium condensates," Phys. Rev. Lett. **121**, 235302 (2018).
26. P. Cristofolini, A. Dreismann, G. Christmann, G. Franchetti, N. Berloff, P. Tsotsis, Z. Hatzopoulos, P. Savvidis, and J. Baumberg, "Optical superfluid phase transitions and trapping of polariton condensates," Phys. Rev. Lett. **110**, 186403 (2013).
27. A. Askitopoulos, H. Ohadi, A. Kavokin, Z. Hatzopoulos, P. Savvidis, and P. Lagoudakis, "Polariton condensation in an optically induced two-dimensional potential," Phys. Rev. B **88**, 041308 (2013).
28. A. V. Yulin, A. S. Desyatnikov, and E. A. Ostrovskaya, "Spontaneous formation and synchronization of vortex modes in optically induced traps for exciton-polariton condensates," Phys. Rev. B **94**, 134310 (2016).
29. Y. Sun, P. Wen, Y. Yoon, G. Liu, M. Steger, L. N. Pfeiffer, K. West, D. W. Snoke, and K. A. Nelson, "Bose-Einstein condensation of long-lifetime polaritons in thermal equilibrium," Phys. Rev. Lett. **118**, 016602 (2017).
30. A. Askitopoulos, K. Kalinin, T. C. H. Liew, P. Cilibrizzi, Z. Hatzopoulos, P. G. Savvidis, N. G. Berloff, and P. G. Lagoudakis, "Nonresonant optical control of a spinor polariton condensate," Phys. Rev. B **93**, 205307 (2016).
31. L. Pickup, K. Kalinin, A. Askitopoulos, Z. Hatzopoulos, P. Savvidis, N. G. Berloff, and P. Lagoudakis, "Optical bistability under nonresonant excitation in spinor polariton condensates," Phys. Rev. Lett. **120**, 225301 (2018).
32. S. Alyatkin, J. D. Töpfer, A. Askitopoulos, H. Sigurdsson, and P. G. Lagoudakis, "Optical control of couplings in polariton condensate lattices," Phys. Rev. Lett. **124**, 207402 (2020).
33. T. W. Kibble, "Topology of cosmic domains and strings," J. Phys. A **9**, 1387 (1976).
34. T. W. Kibble, "Some implications of a cosmological phase transition," Phys. Rep. **67**, 183–199 (1980).
35. W. H. Zurek, "Cosmological experiments in superfluid helium?" Nature **317**, 505–508 (1985).
36. W. H. Zurek, "Cosmological experiments in condensed matter systems," Phys. Rep. **276**, 177–221 (1996).
37. B. Damski and W. H. Zurek, "Soliton creation during a Bose-Einstein condensation," Phys. Rev. Lett. **104**, 160404 (2010).
38. C. Bäuerle, Y. M. Bunkov, S. Fisher, H. Godfrin, and G. Pickett, "Laboratory simulation of cosmic string formation in the early universe using superfluid $^3$He," Nature **382**, 332 (1996).
39. V. Ruutu, V. Eltsov, A. Gill, T. Kibble, M. Krusius, Y. G. Makhlin, B. Placais, G. Volovik, and W. Xu, "Vortex formation in neutron-irradiated superfluid $^3$He as an analogue of cosmological defect formation," Nature **382**, 334–336 (1996).
40. M. J. Bowick, L. Chandar, E. A. Schiff, and A. M. Srivastava, "The cosmological Kibble mechanism in the laboratory: string formation in liquid crystals," Science **263**, 943–945 (1994).
41. A. Maniv, E. Polturak, and G. Koren, "Observation of magnetic flux generated spontaneously during a rapid quench of superconducting films," Phys. Rev. Lett. **91**, 197001 (2003).
42. C. N. Weiler, T. W. Neely, D. R. Scherer, A. S. Bradley, M. J. Davis, and B. P. Anderson, "Spontaneous vortices in the formation of Bose–Einstein condensates," Nature **455**, 948 (2008).
43. K. Staliunas and V. J. Sanchez-Morcillo, *Transverse Patterns in Nonlinear Optical Resonators* (Springer, 2003), Vol. **183**.
44. I. S. Aranson and L. Kramer, "The world of the complex Ginzburg-Landau equation," Rev. Mod. Phys. **74**, 99–143 (2002).
45. L. Carr and C. W. Clark, "Vortices and ring solitons in Bose-Einstein condensates," Phys. Rev. A **74**, 043613 (2006).
46. P. G. Kevrekidis, D. J. Frantzeskakis, and R. Carretero-González, *Emergent Nonlinear Phenomena in Bose-Einstein Condensates: Theory and Experiment* (Springer, 2007), Vol. **45**.
47. N. G. Berloff and C. F. Barenghi, "Vortex nucleation by collapsing bubbles in Bose-Einstein condensates," Phys. Rev. Lett. **93**, 090401 (2004).
48. V. N. Gladilin and M. Wouters, "Multivortex states and dynamics in nonequilibrium polariton condensates," J. Phys. A **52**, 395303 (2019).
49. V. N. Gladilin and M. Wouters, "Interaction and motion of vortices in nonequilibrium quantum fluids," New J. Phys. **19**, 105005 (2017).
50. A. Askitopoulos, L. Pickup, S. Alyatkin, A. Zasedatelev, K. G. Lagoudakis, W. Langbein, and P. G. Lagoudakis, "Giant increase of temporal coherence in optically trapped polariton condensate," arXiv preprint arXiv:1911.08981 (2019).
51. A. Amo, D. Sanvitto, F. Laussy, D. Ballarini, E. Del Valle, M. Martin, A. Lemaitre, J. Bloch, D. Krizhanovskii, M. Skolnick, and C. Tejedor, "Collective fluid dynamics of a polariton condensate in a semiconductor microcavity," Nature **457**, 291–295 (2009).
52. Y. Kawaguchi and T. Ohmi, "Splitting instability of a multiply charged vortex in a Bose-Einstein condensate," Phys. Rev. A **70**, 043610 (2004).
53. L. M. Pismen and L. M. Pismen, *Vortices in Nonlinear Fields: From Liquid Crystals to Superfluids, From Non-equilibrium Patterns to Cosmic Strings* (Oxford University, 1999), Vol. **100**.
54. N. Berloff and B. V. Svistunov, "The turbulent matter field of ultracold atoms," Physics **2**, 61 (2009).
55. G. E. Volovik, "On the Kelvin-Helmholtz instability in superfluids," J. Exp. Theor. Phys. Lett. **75**, 418–422 (2002).
56. H. Takeuchi, N. Suzuki, K. Kasamatsu, H. Saito, and M. Tsubota, "Quantum Kelvin-Helmholtz instability in phase-separated two-component Bose-Einstein condensates," Phys. Rev. B **81**, 094517 (2010).
57. R. Hänninen and A. W. Baggaley, "Vortex filament method as a tool for computational visualization of quantum turbulence," Proc. Natl. Acad. Sci. USA **111**, 4667–4674 (2014).
58. P. M. Lushnikov and N. M. Zubarev, "Exact solutions for nonlinear development of a Kelvin-Helmholtz instability for the counterflow of superfluid and normal components of Helium II," Phys. Rev. Lett. **120**, 204504 (2018).
59. T. Frisch, Y. Pomeau, and S. Rica, "Transition to dissipation in a model of superflow," Phys. Rev. Lett. **69**, 1644 (1992).
60. M. Leadbeater, T. Winiecki, and C. S. Adams, "Effect of condensate depletion on the critical velocity for vortex nucleation in quantum fluids," J. Phys. B **36**, L143–L148 (2003).